InGaAs PV DEVICE DEVELOPMENT FOR TPV POWER SYSTEMS

David M. Wilt, Navid S. Fatemi, and Richard W. Hoffman, Jr.
Essential Research, Inc.
Cleveland, Ohio

Phillip P. Jenkins, David J. Brinker, and David Scheiman
NYMA, Inc.
Brook Park, Ohio

Roland Lowe
Kent State University
Kent, Ohio

and

Donald Chubb
NASA Lewis Research Center
Cleveland, Ohio

SUMMARY

Indium Gallium Arsenide (InGaAs) photovoltaic devices have been fabricated with bandgaps ranging from 0.75 eV to 0.60 eV on Indium Phosphide (InP) substrates. Reported efficiencies have been as high as 11.2% (AM0) for the lattice matched 0.75 eV devices. The 0.75 eV cell demonstrated 14.8% efficiency under a 1500°K blackbody with a projected efficiency of 29.3%. The lattice mismatched devices (0.66 and 0.60 eV) demonstrated measured efficiencies of 8% and 6% respectively under similar conditions. Low long wavelength response and high dark currents are responsible for the poor performance of the mismatched devices. Temperature coefficients have been measured and are presented for all of the bandgaps tested.

INTRODUCTION

Research in thermophotovoltaic (TPV) power systems has persisted for many years, driven by high projected thermal to electric system efficiencies.(ref. 1,2) Several variants of TPV systems have emerged with the principal difference being the method of thermal to radiant energy conversion. In blackbody based systems an emitter material is heated to produce broadband radiation. Unfortunately, much of the emitted energy is below the bandgap of the photovoltaic cell, therefore these systems must include some type of spectrum shaping element. This element must efficiently recycle the low energy photons back to the emitter in order to obtain high system efficiencies.

The other method of producing photons from thermal sources is based on selective emitters. These materials emit energy in a narrow spectral band when heated, eliminating the need for additional spectrum shaping elements. Chubb, et al, have demonstrated rare earth doped Yttrium Alumina Garnets (YAG) crystals with good selective emission properties.(ref. 3) Common to all TPV systems designed for operation at moderate temperatures (< 1500°K) is the need for a low bandgap photovoltaic device. For blackbody based systems, the optimum bandgap is dependant upon the operating temperature of the emitter and of the cell. For an emitter temperature of 1500°K, Woolf (ref. 2) has calculated that the optimum bandgap ranges from 0.52 eV to 0.82 eV depending upon the cell temperature. The optimum bandgap for selective emitter based systems depends upon the composition of the selective emitter (ref. 1).

The original work in TPV utilized standard silicon solar cells. The high bandgap of silicon (Eg = 1.1 eV) limited the systems to very high emitter temperatures (> 2000°K). Radio-isotope and conventionally fueled heat sources operate at much lower temperatures, requiring lower bandgap photovoltaic devices. Indium Gallium Arsenide ($In_xGa_{1-x}As$) is a direct bandgap semiconductor material that has a bandgap ranging from 0.35 eV to 1.42 eV depending on the In/Ga ratio. $In_{.53}Ga_{.47}As$ solar cells (Eg =0.75 eV), with efficiencies of up to 11.2% (AM0), have been fabricated on lattice matched indium phosphide (InP) substrates (ref. 4).

EXPERIMENT

$In_xGa_{1-x}As$ device structures were grown by Organo Metallic Vapor Phase Epitaxy (OMVPE) in a horizontal, low pressure reactor designed and constructed at NASA Lewis. The source gases consisted of trimethyl gallium, trimethyl indium, arsine (100%), phosphine (100%), diethyl zinc, and silane diluted in hydrogen. Typical growth conditions were: 620°C growth temperature, 190 torr reactor pressure, V/III ratio of 75, and carrier gas flow rate of 3.5 std. l/min. The InP substrates were zinc doped ($p = 4e18\ cc^{-1}$), oriented (100) and used as received from the vendor. A co-flow of arsine and phosphine was used at the time of crossover from InP growth to InGaAs growth. The co-flow lasted 10 sec. and was used to protect the InP substrate from decomposition until the InGaAs had formed a continuous coverage. The growth rate of InP was 6.1 Å/sec and the growth rate of InGaAs was 8.1 Å/sec.

Device structures for the 0.75, 0.66 and 0.6 eV $In_xGa_{1-x}As$ devices are shown in figure 1. The lattice matched InGaAs device (0.75 eV) incorporated a very thick (1.5 μm) InP window layer to reduce the series resistance. Modeling predicts a very high short circuit current density from this device ($4.7\ A/cm^2$) under a 1500°K blackbody emitter (approximately equivalent to 170x AM0), therefore reduction of resistive losses through window layer design and front contact grid design will be very important. Losses due to absorption in the thick InP window layer are minimal under a 1500°K blackbody.

The lattice mismatched devices (Eg = 0.66 and 0.6 eV) incorporate step graded buffer layers between the InP substrate and the cell structure. These layers attempt to minimize the density of threading dislocations in the active device layers. An extensive examination of the effect of the grading structure on the performance of lattice mismatched devices is planned. Due to the lattice mismatch (0.74% and 1.2%) of the 0.66 and the 0.6 eV material, thin InP window layers were used in these devices. Alternate window layer materials based on InAsP and AlInAs are under development to allow the incorporation of thick window layers for the reduction of series resistance.

The devices were processed using standard thermal evaporation and photolithographic techniques. The lattice mismatched cells were processed with a higher coverage front grid pattern to partially offset the limitations imposed by the high sheet resistance of the devices. Single layer anti-reflective coatings of Ta_2O_5 were roughly matched to the expected illumination source.

RESULTS

Figure 2 shows the AM0 I-V data for the three different bandgap InGaAs devices without AR coatings. The large change in J_{sc} with bandgap is not directly related to bandgap, as might be thought. The 0.75 eV cell has a thick (1.5 μm) InP window layer that dramatically reduces the AM0 J_{sc}, which can be seen in the external quantum efficiency (QE) data of figure 3. Dark diode measurements of the devices demonstrated that they were all diffusion limited, with diode ideality factors of ~1. The dark current showed a large dependence on lattice mismatch as can be seen in table 1.

The external QE measurements (figure 3) were taken after Ta_2O_5 AR coating deposition. Unfortunately, our equipment limits the measurements to 1.9 μm, at which point the 0.6 and 0.66 eV cells are still operating. The roll off of the mismatched InGaAs devices at the longer wavelengths is expected due to the deep absorption depth of the low energy photons and the short minority carrier lifetimes expected in the heavily dislocated material. Optimization of base thicknesses, doping levels and lattice grading structures should improve the long wavelength response.

The test devices were mounted on fixtures to facilitate their testing under blackbody and selective emitter illumination. The test fixture incorporated 4-wire connections for independent current and voltage measurement and a thermocouple mounted under the cell to monitor the operating temperature. An electric furnace, used for selective emitter development, was used as a 1500°K blackbody illumination source (fig. 4). Its' emissivity had previously been determined to be > 0.95. Calculations indicate that total emitted power from the black body should be 26.5 W/cm^2, although measurements of the actual emitted power were only 3.0 W/cm^2 where the cells were mounted. This difference is attributed to the reduction in view factor which results from the 3.6 cm separating the cell from the furnace viewport.

The 0.75 eV cell was also measured under the illumination of an Er-YAG selective emitter at 1500°K (fig. 4). The measured output power from the selective emitter was 1.9 W/cm^2 at the cell test distance. This value is down from the 5.7 W/cm^2 value calculated from the measured selective emitter (SE) spectral emmisivity data. Difficulties were experienced in accurately determining the surface temperature of the SE and in keeping the entire exposed surface at a uniform temperature. Due to these errors we will not be reporting efficiencies for the InGaAs devices under SE illumination.

The results of the test devices under the blackbody illumination are listed in table 2. As expected, the cell efficiency without filters to recycle the sub-bandgap photons is very low. The 0.75eV cell is only able to absorb 16.8% of the total incident radiative energy. If the sub-bandgap portion of the spectrum is eliminated from the measurement, the efficiency increases to 14.8%. An efficiency of 29.3% was predicted for this device. Those predictions assumed the illumination of the cell by a perfect black body (emissivity =1) at 1500°K with a view factor of 1, and used the measured SR and dark diode characteristics of the actual test device. The discrepancy in efficiencies is largely attributable to the low intensity of the actual measurement compared to the calculated spectrum. The actual cell generated 277 mA/cm^2 of short circuit current, whereas the integration of the SR with the perfect blackbody spectrum predicted a J_{sc} of 4.7 A/cm^2. Achieving this optical coupling in actual practice will obviously entail the incorporation of optical concentrating elements, given the necessity of separating the emitter from the cell for thermal management reasons. Another reason for the large difference in the predicted vs. measured cell efficiency was a slight degradation in the cell performance after mounting on the test fixture. The cell had a smaller shunt resistance after mounting, leading to a reduction in the fill factor. Additional experience in mounting devices should eliminate this problem. Calculated cell efficiencies for the 0.66 and 0.6 eV devices is not included due to the incomplete QE data for these devices.

Cell performance as a function of cell temperature is shown in figures 5-7 and table 3 under blackbody illumination. The temperature coefficients of V_{oc} were very constant at -1.6 mV/°C for all of the bandgaps tested. As expected, the J_{sc} increased with increasing cell temperature, due to bandgap narrowing. An interesting feature of the lattice mismatched devices is the peak in the J_{sc} at a cell temperature of ~70°C. We believe that this is caused by increased recombination in the bulk as the temperature increases. The effect is more pronounced in the greater lattice mismatched 0.60 eV cell compared to the 0.66 eV cell. This indicates that the recombination mechanism may be related to the misfit and threading dislocations present in the mismatched InGaAs.

Figure 8 shows the temperature dependence for the 0.75 eV cell under the Er-YAG selective emitter. The small change in J_{sc} with increasing temperature indicates that the SE has very little emission outside of the Er related emission band.

CONCLUSIONS

Lattice matched InGaAs has been demonstrated to have excellent potential for application in TPV power systems. Non-optimized device structures have projected efficiencies approaching 30% under 1500°K blackbody illumination. Lattice mismatched InGaAs devices offer the ability to "tune" the photovoltaic device response to correspond to the emission band of the illumination source. Initial results indicate that poor long wavelength response and high dark currents need to be addressed before these devices are feasible. The effect of buffer layer design on device performance must be examined for lattice mismatched devices. We are also planning to examine the effectiveness of hydrogen passivation for reducing the deleterious effects of threading dislocations. Design of an actual TPV system will require many trade off studies. It may turn out to be be preferable to use an efficient photovoltaic device which is not optimally tuned to the emission source rather than a poor performance device that is tuned to the source.

REFERENCES

1. D. Chubb, R. Lowe and D. Flood, NASA TM 105755 (1992)
2. L.D. Woolf, Solar Cells **1 9**, 19 (1986).
3. R.L. Lowe, D.L. Chubb, S.C. Farmer and B.S. Good, "Rare Earth Garnet Selective Emitter", Submitted to Appl. Phys. Lett. (1994)
4. D.M. Wilt, N.S. Fatemi, R.W. Hoffman, Jr., et al, Appl. Phys. Lett. **6 4** (18), p. 2415 (1994)

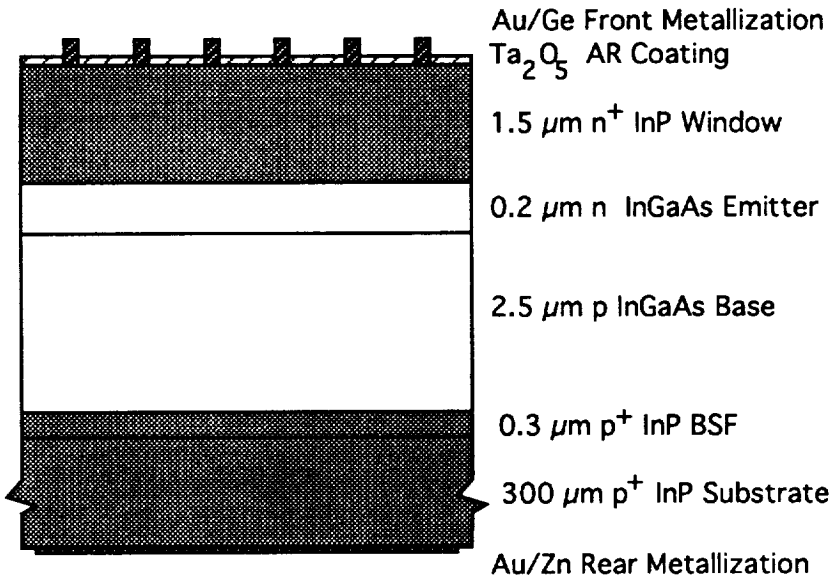

0.75 eV InGaAs Cell Structure

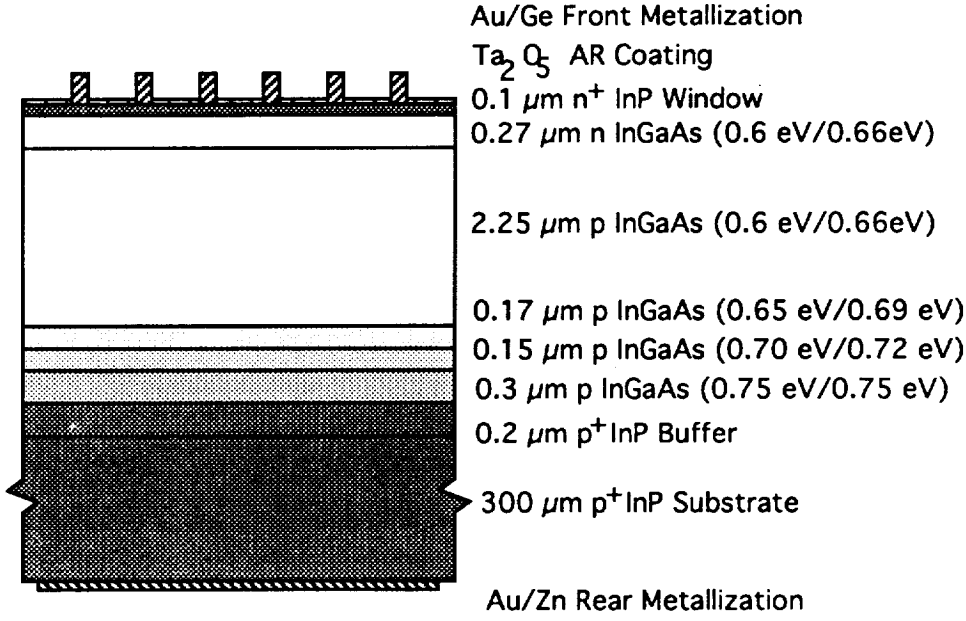

0.60 eV/0.66eV InGaAs Cell Structure

Figure 1 - InGaAs TPV cell Structures

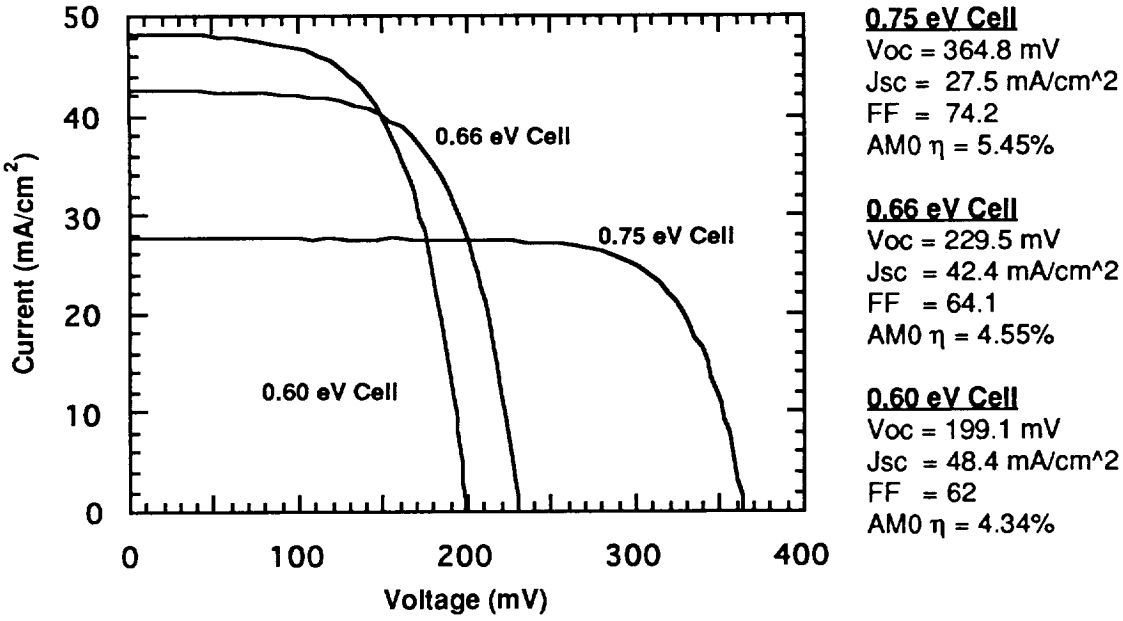

Figure 2 - AM0 I-V data for InGaAs solar cells without AR coatings.

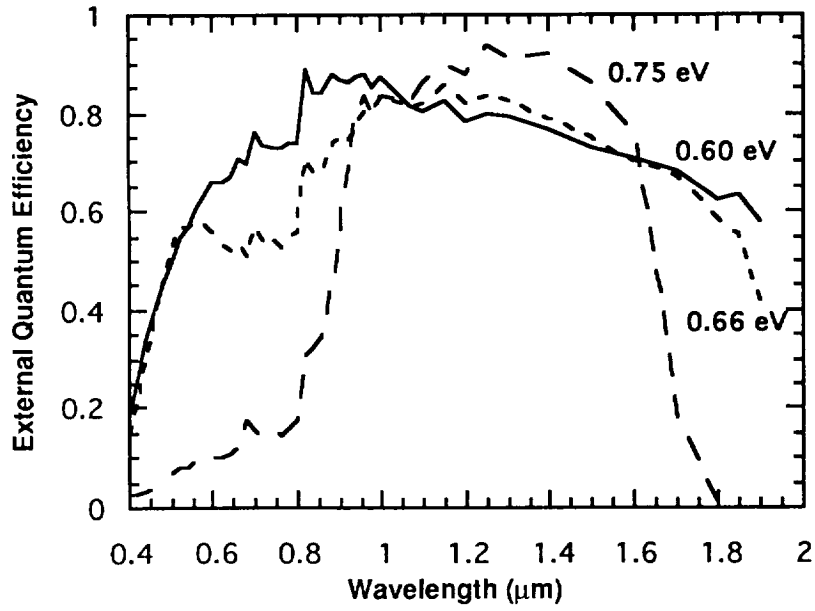

Figure 3 - External QE measurements of AR Coated InGaAs Devices

Bandgap (eV)	A	J01 (A/cm^2)	Rs (Ω)	Rsh (Ω)
0.75	1.01	3.6e-8	0.453	3.4e3
0.66	0.99	6.5e-6	0.431	2.5e3
0.60	0.96	2.2e-5	0.387	8.0e2

Table 1 - Dark diode data for InGaAs devices at 25 °C

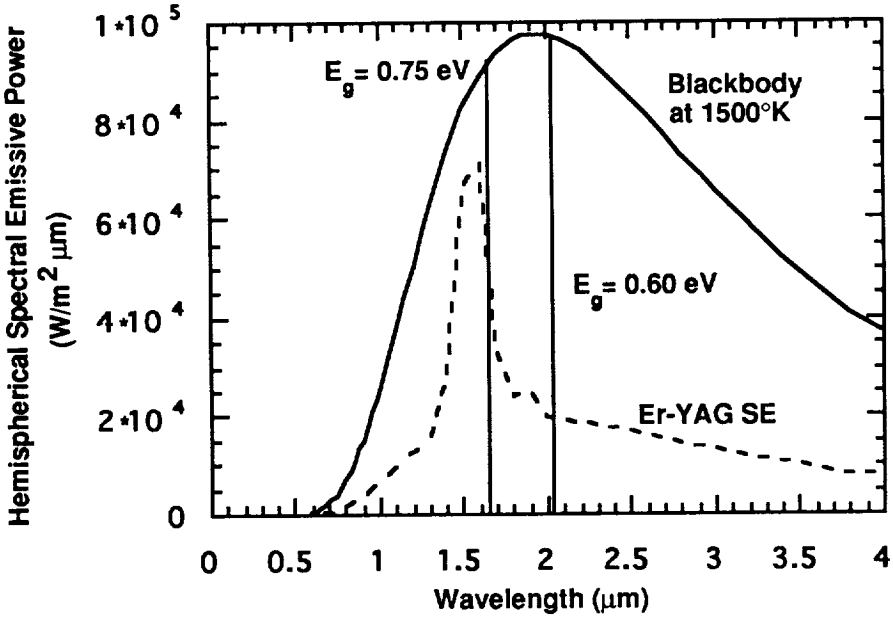

Figure 4 - Blackbody and Er-YAG Selective Emitter Spectrum at 1500 °K.

Bandgap (eV)	Measured Cell Efficiency w/o filter	Measured Cell Efficiency assuming a perfect filter	Calculated Cell Efficiency using Measured SR
0.75	2.5% #	14.8%	29.3%
0.66	1.9% #	8.0%	
0.60	1.9% #	6.0%	

Cell Temperature = 34°C

Table 2 - Performance of InGaAs Devices under Blackbody Illumination

Bandgap (eV)	(1/Jsc)(dJsc/dT) (x e-3/°C)	(1/Voc)(dVoc/dT) (x e-3/°C)	(1/FF)(dFF/dT) (x e-3/°C)	(1/Pmax)(dPmax/dT) (x e-3/°C)	Linear Temperature Range (°C)
0.75	1.99	4.20	2.32	4.67	30-60
0.66	3.18	7.44	6.39	1.01	30-60
0.60	3.04	6.97	5.87	9.46	30-70

Table 3 - Temperature Coefficients for InGaAs Cells Under 1500°K Blackbody Illumination

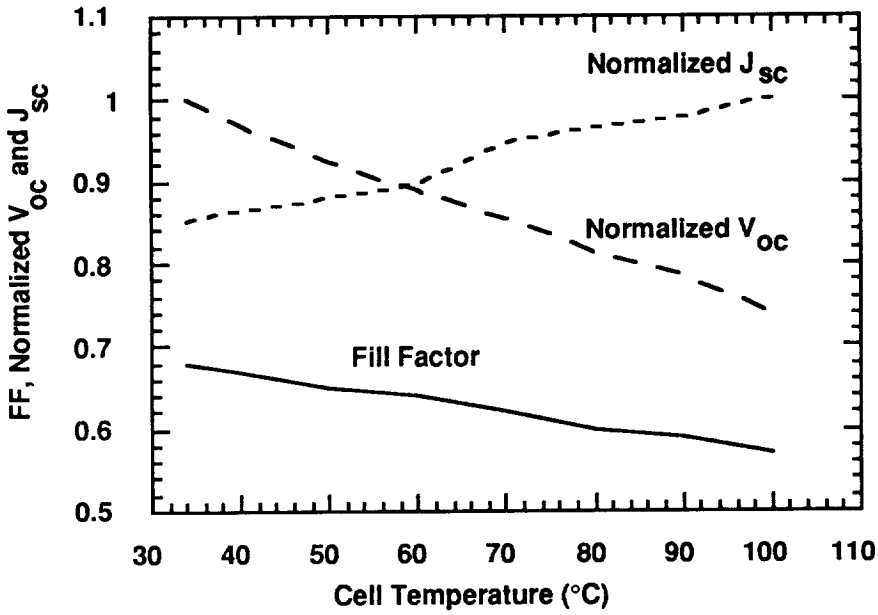

Figure 5 - 0.75 eV InGaAs Cell Performance vs. Temperature
Under 1500°K Blackbody Illumination

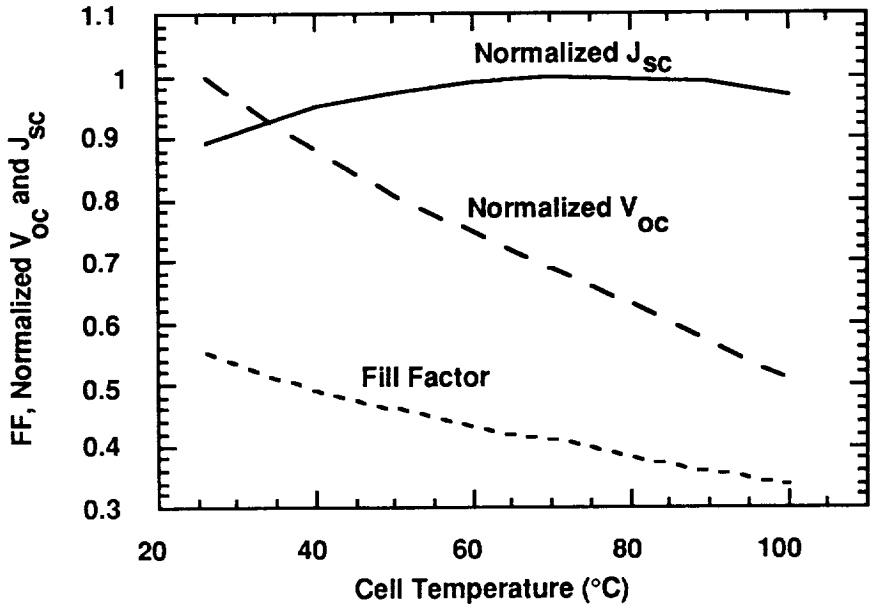

Figure 6 - 0.66 eV InGaAs Cell Performance vs. Temperature
Under 1500°K Blackbody Illumination

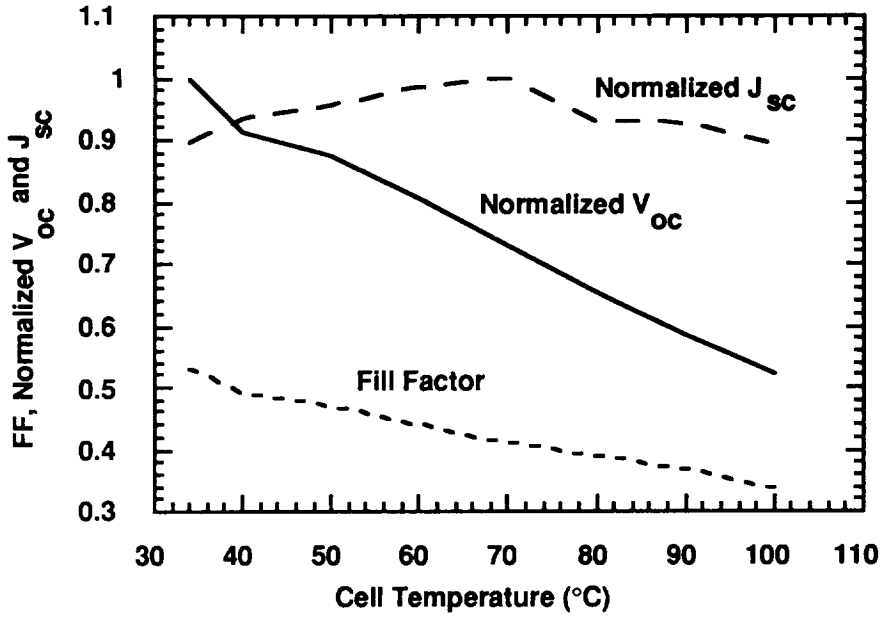

Figure 7 - 0.60 eV InGaAs Cell Performance vs. Temperature
Under 1500°K Blackbody Illumination

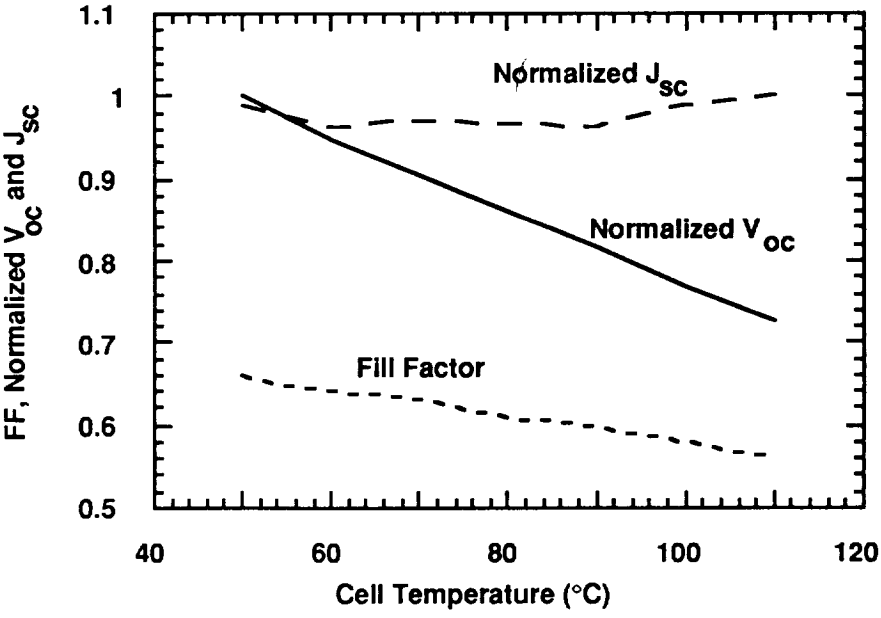

Figure 8 - 0.75 eV InGaAs Cell Performance vs. Temperature
Under 1500°K Er-YAG Selective Emitter